Role of Dissolved CO in the Solution on the Origin of CO Pre-oxidation on Pt(111)-Type Electrodes

Manuel J. S. Farias*,†, Benedicto A. V. Lima‡, Germano Tremiliosi-Filho§ and Enrique Herrero‖

†*Departamento de Química, Universidade Federal do Maranhão, Avenida dos Portugueses, 1966, CEP 65080-805, São Luís, Maranhão, Brazil*

‡*Universidade Federal do Maranhão, Campus Universitário de Grajaú, Avenida Aurila Maria Santos Barros de Sousa, CEP 65940-000, Grajaú, Maranhão, Brazil*

§*Instituto de Química de São Carlos, Universidade de São Paulo, Av. Trabalhador Sãocarlense, 13560-970, São Carlos, São Paulo, Brazil*

‖*Instituto de Electroquímica, Universidad de Alicante, Ap. 99, E-03080, Alicante, Spain*

Abstract

In voltammetric CO stripping experiments in acid media, CO pre-oxidation usually takes place on catalysts with a high density of surface defects, obeyed the conditions of full CO_{ads} layer formation at suitable low potentials into the "hydrogen region" and, importantly, CO traces in the bulk of the solution is required. This study aims to interrogate that. The electro-oxidation of CO was voltammetrically conducted applying different scan rates, employing Pt(111) terraced surfaces and full CO coverage equilibrated with different content of dissolved CO in the bulk of an acid quiescent solution; also experiments were performed in which CO_{ads} was present only on the (110)-type steps in a CO-free solution. It was found that: (1) slopes of peak potentials of CO pre-oxidation *versus* the logarithm of scan rates were smaller for higher CO contents in the solution; (2) charge density of CO pre-oxidation was higher for slower scan rate; (3) CO pre-oxidation takes place at low potentials where the (110)-type step sites were inactive in the catalysis of CO electro-oxidation. We conclude that, in such a quiescent solution, the content of dissolved CO in the bulk of the solution determines the magnitude and the shape of the curve of the CO pre-oxidation. This can be understandable in terms of prompt provision of CO molecules from the solution (diffusion layer) to surface active sites, that is, the most active sites, released during the CO pre-oxidation. In the CO pre-oxidation on Pt(111) terraced surfaces, the most active sites lie at

the bottom of (111) terraces. The results provide evidence that, in presence of CO traces in the bulk of the solution, on one hand, the pre-oxidation of CO involves the diffusion-limited electro-oxidation of bulk CO at most active sites released during the CO pre-oxidation process. On the other hand, the main CO electro-oxidation peak is a typical behavior of a surface-confined process. Our proposition applies to Pt electrodes in acidic medium.

Keywords: electrocatalysis, CO electro-oxidation, crystalline Pt surfaces, active sites.

*Corresponding Author: manueljsfarias@gmail.com (Manuel J. S. Farias)
Phone: +55 98 3301 8246.

1. Introduction

In the field of heterogeneous electrocatalysis, platinum is one of the known catalytic materials for which the CO electro-oxidation better behaves as a sensitive reaction to the surface structure. The adsorption and electro-oxidation of CO are prototypical examples of surface probe reactions [1, 2]. Interestingly, the CO electro-oxidation reaction presents very intriguing facets. For instance, the electrochemical oxidation of the CO_{ads} layer (in the absence of CO in the bulk of the solution), usually requires high overpotentials (ca. 0.8 V) to start on pure Pt electrodes, when compared to the standard potential for the reaction $CO_{(g)} + H_2O_{(l)} \rightleftarrows CO_{2(g)} + 2H^+ + 2e^-$, which is E^0 = -0.104 V_{SHE} [3]. In fact, at low overpotentials, the electro-oxidation of CO shows a sluggish kinetic reaction rate [4-6]. However, it was accidentally observed in some experiments of CO_{ads} stripping (and bulk CO electro-oxidation as well) that the reaction initiates at lower overpotentials, in a slow kinetic process known as CO pre-oxidation. It has been observed in several types of platinum electrodes in acid solution that pre-oxidation only occurs if the solution contains traces of dissolved CO [7]. In this respect, there is still a need to elucidate a possible underlying mechanism that explains the role played by CO in the solution in the emergence of the CO pre-oxidation on Pt electrodes in acid solutions. This study focuses on this question.

Due to its importance in terms of catalysis, many publications address the issue of CO pre-oxidation, in particular on Pt and Pt-based electrodes [7-23]. Generally, the divergences that exist on the topic concern the mechanism underlying the CO pre-oxidation phenomenon. However, the experimental control of conditions required for the CO pre-oxidation to be a reproducible phenomenon has not always been well understood and, perhaps for that reason, there is so much divergence on this subject. Herein, we will describe how the CO pre-oxidation proceeds in voltammetric experiments, specifically, CO stripping on Pt electrodes in acid media. So, in CO stripping experiments, in which a CO_{ads} layer is formed on the electrode surfaces and non-adsorbed CO is (partially) eliminated from the bulk of the solution, the voltammetric CO electro-oxidation usually starts at very low overpotentials developing a small pre-wave that usually separates from the main CO electro-oxidation process [9, 10, 14]. This slow kinetics process is called CO pre-oxidation. It is worth highlighting that, for bulk CO oxidation and under forced convection (using the hanging meniscus rotating disk electrode configuration), it is not possible to differentiate the pre-oxidation from the main oxidation process because the adsorption of CO molecules from the

bulk of the solution retards the ignition process, so that it occurs simultaneously with the electro-oxidation of CO from the solution [24, 25]. When a CO_{ads} layer is formed at constant and low potentials, as those in the hydrogen underpotential deposition region, the CO electro-oxidation process starts at very low overpotentials [9, 10]. This is a fact widely corroborated in the literature [14, 26, 27]. Indeed, the CO dosing potential was the first experimental condition observed to be linked to the reproducibility of the CO pre-oxidation [10, 14]. In this line, López-Cudero *et al.* [14] found that high CO coverage and defect-rich catalyst surface are needed for the appearance of the CO pre-oxidation. This was a very interesting finding because it suggests that the CO pre-oxidation is surface-structure sensitive in the sense that defects are required, in addition to both the aforementioned: CO adsorption potential and high CO coverage. Intriguingly, if the three conditions above are met, namely; low CO adsorption potential, high CO coverage, and defect rich catalyst surfaces, the CO pre-oxidation on Pt(111)-type electrode in acidic medium only happens when the bulk of the solution contains at least traces of dissolved CO [7]. This intriguing fact will be investigated in detail, with the solution containing different amounts of dissolved CO, and applying different scan rates for the voltammetric electro-oxidations of the CO on stepped Pt(111)-type surfaces. However, it is worth mentioning that a recent finding revealed that the pre-oxidation of CO is not an exclusive phenomenon of defect-rich catalyst surfaces and it appeared even in the absence of dissolved CO in the solution [23], which increases the complexity of the catalytic mechanisms underlying the phenomenon of the CO pre-oxidation. In this paper, we delimit the study only on cases in which CO pre-oxidation is favored on Pt surfaces rich in defects, and obey specific conditions of potential for CO adsorption.

Regarding the defects on catalyst surface, the rate of the CO electro-oxidation reaction on stepped surfaces with (111) terraces *very often* increases as the density of surface steps (defects) increases [28]. In this situation, it is normally expected that the defects on the surface are directly involved as active sites in the enhancement of the reaction rate. However, controlled experiments based on labeling specific active sites with the reaction intermediates – adsorbed ^{13}CO on top of the surface defects – have revealed that steps (or defects) do not chemically or directly participate as active sites in the catalytic enhancement of CO electro-oxidation reaction [29]. Instead, defects on the surfaces have an indirect involvement in the enhancement, because they tune the catalytic properties on (111) terraces so that a higher catalytic activity for CO electro-oxidation reaction is observed. It should be noted that this

catalytic behavior is absent on the "infinite" (or perfect) (111) terraces, (Pt(111) basal plane), explaining why the presence of surface defects usually increases the catalytic activity. Another relevant aspect that is observed for a structure sensitive reaction such as the CO electro-oxidation reaction is that the measured faradaic current density involving the CO electro-oxidation reaction is the result of the sum of the activity of the different sites working with very different efficiencies or abilities [29]. Conceptually, for reactions that are surface structure-sensitive, if the different sites (or facets) on the catalyst surface act as active sites, it is not expected that such different sites are active (or become activated) requiring the same driving force or overpotentials (in the case of electrochemical reactions). Consequently, if the different sites require a different driven force to be activated, it is then expected that some active sites may deliver the reaction outcome while other ones keep entirely inactivated or even poisoned by reactants and/or reaction intermediates. This is especially important at low overpotentials, that is, when the driving force is small. Conceptually, this is a very interesting subject to be investigated in heterogeneous electrocatalysis, and for that, the electro-oxidation of CO is a very suitable surface probe reaction. This type of heterogeneity of active sites on Pt(111) terraced surfaces consisting of (110)-type steps and (111)-type terraces will be investigated employing the CO electro-oxidation reaction as a surface probe reaction in presence of CO traces in the bulk of a quiescent electrolyte solution. This allows studying the role of surface defects together with the possible role played by CO in the bulk of the solution in the electro-oxidation of CO at low overpotentials.

The aim of the study was to provide further insights about the role of CO in the bulk of the solution on pathways of electro-oxidation reaction of CO at low overpotentials.

2. Experimental Section

In this study, bead-type electrodes were used as working electrodes. Specifically, the following crystalline surfaces were used: Pt(111), Pt(13 13 12), and Pt(776). Pt(13 13 12) and Pt(776) are stepped surfaces, which, according to the Lang-Joyner-Somorjai nomenclature [30], belong to the Pt(s)-[(n – 1)(111)×(110)] series, in which n refers to the atomic width of the (111) terraces. Under this notation, the corresponding Miller index for this series is (n, n, n – 2), being each stepped surface individually represented as:

$$\text{Pt(13 13 12)} \equiv \text{Pt(s)-[25(111)×(110)]}, \text{with } n - 1 = 25$$

$$\text{Pt(776)} \equiv \text{Pt(s)-[13(111)×(110)]}, \text{ with } n - 1 = 13$$

Thus, the Pt(13 13 12) and Pt(776) electrodes have 25, and 13 atom-wide (111) terraces, respectively, separated by (110) monoatomic steps. The step density for these surfaces is defined as the number of steps per unit length in the plane of the terrace, $\rho_{(hkl)}$, in cm^{-1}. The oriented surface area (A) of each electrode was: Pt(111), $A \simeq 4.53$ mm^2; Pt(Pt(13 13 12), $A \simeq 3.33$ mm^2; Pt(776), $A \simeq 3.66$ mm^2. Current densities have been calculated using these areas.

As standard procedure, the working electrodes were annealed in a butane/air flame and then cooled in a reducing Ar/H_2 atmosphere (free of oxygen) [31]. A Pt wire was used as a counter electrode, which was annealed in a butane/air flame several times and washed with ultra-pure water before use. As a reference electrode, a reversible hydrogen electrode was used, and all the potentials were quoted against this reference electrode. The temperature of the experiments was 25 ± 1.0 °C (room temperature in the laboratory).

Solutions were prepared in ultrapure water (18.2 MΩ cm) and $HClO_4$ (Aldrich, 70 %). The electrochemical technique employed in this study was cyclic voltammetry. For this technique, the potential of the electrode was controlled using a waveform generator (Model 175, EG&G PARC) together with a potentiostat (Model 551, Amel) and a digital recorder (Model ED 401, eDAC). For comparison between experiments recorded at different scan rates, the curves of current density *vs* potential have been divided by the scan rate, v, since peak currents increases almost linearly with the scan rate.

To register the voltammetric CO stripping experiments, the CO (N47, Alpha Gaz) gas was admitted in the electrochemical cell by bubbling it (flow of ~200 mL/min in all experiments) through the solution for 5 minutes, at a fixed potential of 0.1 V (unless otherwise noted). Next, non-adsorbed CO was (partially) eliminated from the bulk of the solution by bubbling Ar (N50, Alpha Gaz) with a flow of ~150 mL/min for controlled times ranging from 0 (which implies that the solution is CO saturated) to 30 minutes (which implies that non-adsorbed CO is completely eliminated from the bulk of the solution). In this respect, all experiments were carried out using the same electrochemical cell, always employing a similar quantity (volume) of solution. In the case of Ar flow for 18 minutes, the consecutive recording of two voltammograms, that is, the CO stripping profile and its subsequent blank cyclic voltammogram, evidenced the presence of CO in the second voltammetric cycle because the CO partially blocked the hydrogen region in the second cycle, and consequently a small CO electro-oxidation peak appeared at ~0.712 V in the second scan, shown in Figure SI 1.

3. *Results*

3.1. Voltammetric profiles of the electrodes in a CO-free electrolyte

Figure 1 shows the cyclic voltammograms of different Pt single crystal electrodes, namely, Pt(111) basal plane, Pt(13 13 12), and Pt(776), recorded in a 0.1 M $HClO_4$ solution. This figure also includes a hard-sphere model of a Pt(776) stepped surface assigning the different surface sites considered (the top of the step and its corresponding bottom side, and the terrace domain), with information on the charge separation process at the steps, which generated a surface dipole. It should be noted that the quality of the voltammograms in Figure 1 indicates that the crystal surfaces were well-ordered and the solution was free of impurities.

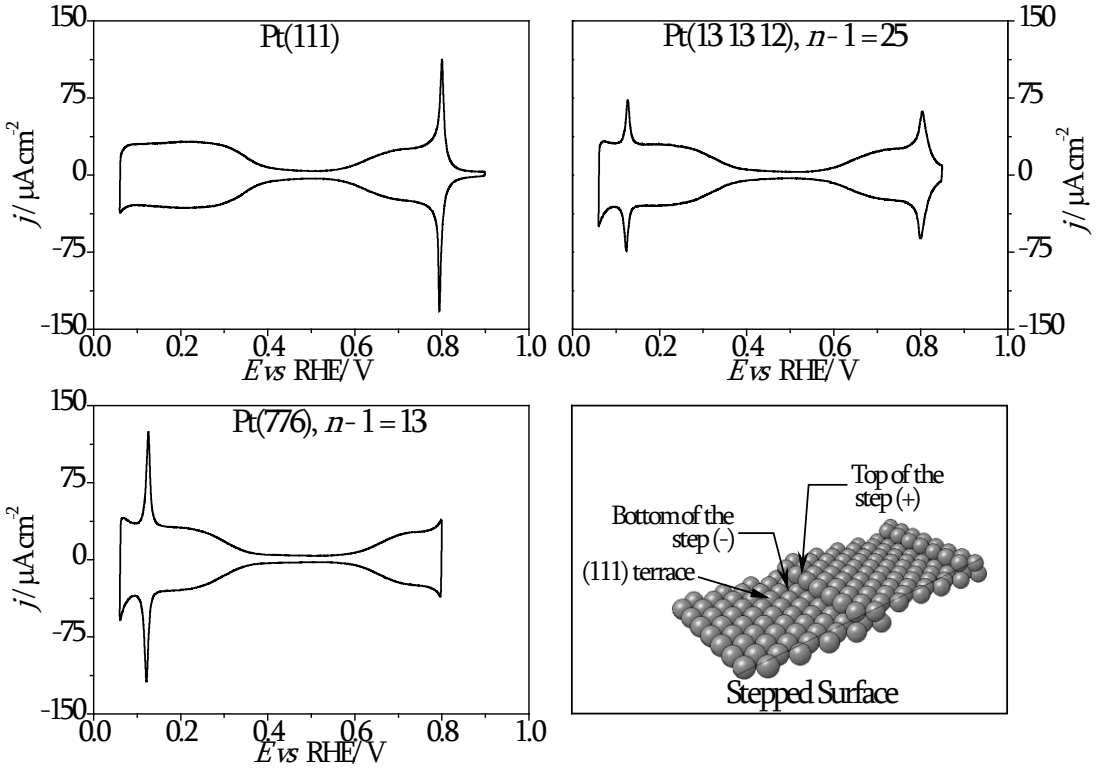

Figure 1. Cyclic voltammograms of Pt(111), Pt(13 13 12) and Pt(776) single crystals electrodes in a 0.1 M $HClO_4$ solution, at a scan rate of 0.05 V s^{-1}. The figure includes a hard model of a stepped surface (drawn using http://surfexp.fhi-berlin.mpg.de/) showing the dipole created on the step.

For Pt(111) surfaces in this electrolyte, the potential of zero total charge is ~0.33 V_{RHE}, and it decreases slightly as defects are introduced into the (111) plane [32]. In this sense and regardless of the crystal surface orientation, it is reasonable to assume that in this supporting electrolyte, the dominant interfacial processes at potentials lower than ~0.33 V are the reversible charge/discharge of the (solvated) proton to form adsorbed hydrogen atom

(H_{ads}). This electrochemical process is also termed as hydrogen underpotential deposition (H_{UPD}), which can be represented simply as $H^+ + e^- + *_{active\ sites} \rightleftarrows H_{ads}$. These reactions are fast, surface-limited, and importantly, are extremely sensitive to the structure of Pt surface sites, allowing to identify the presence and orientation of the terrace and the step/defect sites. This surface structure sensitive behavior of hydrogen adsorption/desorption on Pt electrodes is also useful to identify whether certain types of active Pt surface sites are available or not, as will be detailed below. The signals in the cyclic voltammogram of this surface at potentials above 0.6 V are mainly related to the adsorption/desorption of OH on the electrode surface. For the Pt(111) electrode, the prominent reversible spike at ~0.8 V is very sensitive to the long-range order of the (111) facet and is affected probably by the interactions of adsorbed OH with perchlorate anions and water interfacial molecules [33]. In this sense and as expected (see Figure 1), the features at ~0.8 V decreased as steps (defects) are introduced into the (111) plane.

For stepped Pt surfaces, when the potential window was raised to about 0.9 V_{RHE}, an irreversible change in the voltammogram appeared, indicating the occurrence of a surface restructuring process. For this reason, the upper potential limit for the voltammetric scans decreases as the step density increases (Figure 1). However, for the present study, the most important point is to characterize or to establish the relationships between the surface structure and the electrochemical processes that result in the prominent peaks in the hydrogen region as seen in Figure 1. In this sense, the increase of the surface step density, *i.e.*, when moving from Pt(111) to stepped Pt surfaces – since $\rho_{(111)} << \rho_{(13\ 13\ 12)} < \rho_{(776)}$ – leads to an increase in the intensity (and charge density) of the features at ~0.13 V. These peaks are the fingerprint of hydrogen adsorption/desorption at the top of the (110)-type step orientations (see hard-sphere model in Figure 1), as demonstrated by Clavilier *et al.* [34]. As it can be seen in Figure 1, the peaks at ~0.13 V are absent in the voltammogram of Pt(111) surface, which indicates that this surface is well-ordered. Moreover, in the pH solution (and ionic strength) employed in this study (0.1 M $HClO_4$ with pH ~1.2), the signatures of (100)-type steps should appear at ~0.28 V_{RHE}. None of the voltammograms in Figure 1 exhibits peaks around ~0.28 V_{RHE}, which indicates that all the crystal surfaces used in this study were well-ordered. Any site-selective adsorption process taking place on a Pt stepped surface preferentially blocks either the terraces or the step sites (top of the steps), as it will be shown in the next section.

3.2. Catalytic activity of "infinite" (111)-type terraces and (110)-type steps toward electro-oxidation of CO

Electro-oxidation of CO on well-ordered Pt(111) surfaces are shown in Figure 2. To register these experiments, the potential was fixed at 0.1 V and CO was bubbled through the solution for 5 minutes. After this, the CO gas stream was interrupted, and non-adsorbed CO was partially eliminated from the bulk of the solution by bubbling Ar gas through the solution for 18 minutes. CO stripping experiments at different scan rates were recorded, as shown in Figure 2. As expected [35], the stripping voltammograms of the saturated CO_{ads} layer on the Pt(111) surface presents a single CO electro-oxidation peak. This result shows that the main peak of the electro-oxidation of a CO_{ads} layer adsorbed at 0.1 V on a well-ordered Pt(111) surface is not preceded by a CO pre-oxidation process. It is worth mentioning that a recent publication reports that, for a CO_{ads} layer adsorbed when flame annealed Pt(111) electrode was cooled in a CO atmosphere, the stripping of the CO_{ads} layer presented a prominent CO pre-oxidation process [23], but that experimental condition for the preparation of the CO_{ads} layer was not applied in the present study. For experimental conditions employed in experiments of Figure 2, specifically CO adsorption potentials and partial elimination of non-adsorbed CO, the total CO coverage determined from the integration of the stripping peak (corrected by electric double layer [36]) was $\theta_{CO} \simeq 0.70$. This is similar to results already reported in the literature, evidencing that the total CO_{ads} coverage is also determined by the equilibrium involving CO_{ads} in the compact layer and dissolved CO in the bulk of the solution (partial pressure of CO) [37]. This coverage value is also, within the error of the measurements, the value expected for the CO superstructure $\left(\sqrt{19}\sqrt{19}\right)R23.4^{o}$–13CO ($\theta_{CO} \simeq 0.68$), observed by STM on a Pt(111) electrode in the absence of CO in solution [38].

It is important to highlight that 18 minutes of Ar stream was not enough to completely eliminate CO from the solution. The presence of traces of CO in the bulk of the solution was detected in subsequent cyclic voltammograms (not shown) recorded after CO stripping experiments shown in Figure 2. It should be emphasized that even in the presence of traces of CO in the solution, the CO stripping experiments in Figure 2 do not show any signs of a CO pre-oxidation wave. The inset of Figure 2 shows the Tafel plots of the CO electro-oxidation peak, *i.e.*, the plots of peak potentials *versus* the logarithm of scan rate ($dE_p/d\,log v$) recorded directly from the respective the cyclic voltammograms for scan rate ranging from 0.002 to 0.100 V s^{-1}. The measured Tafel slope is 86 mV dec^{-1}. For the present condition, the

potential scan rate range was restricted from 0.002 to 0.200 V s^{-1}. At higher scan rates, a change in the values of the $dE_p/d\,logv$ slope is observed [21], probably associated with changes in the surface conditions of the electrode at those scan rates.

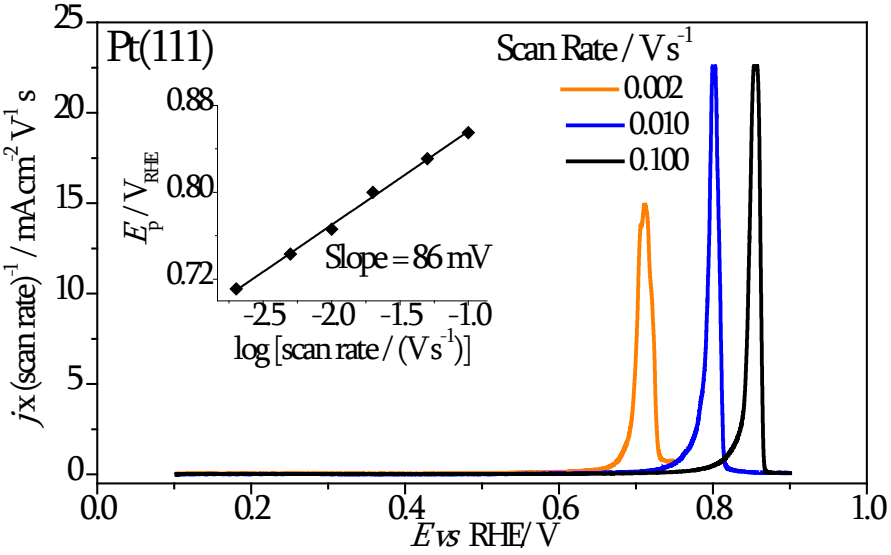

Figure 2. Voltammetric profiles divided by the scan rate of the electro-oxidation of a full CO_{ads} layer on a well-ordered Pt(111) electrode at different scan rates, in 0.1 M $HClO_4$. The inset shows the plot of the peak potentials *versus* the logarithm of the sweep rate. The CO gas was admitted in the cell with the electrode fixed at 0.1 V. The non-adsorbed CO was removed from solution by bubbling Ar gas for 18 min.

The experiments presented in Figure 2 serve to define the catalytic activity of electro-oxidation of CO on well-ordered Pt surfaces, *i.e.*, on a surface consisting of "infinite" (111) terraces. Therefore, in Figure 2 the catalytic activity was evaluated for (111) terraces "free" of the effects coming from surface defects, and it would be a kind of the intrinsic catalytic activity to the (111) terrace sites. The experiments in Figure 2 confirmed that, under those experimental conditions with respect to the CO_{ads} layer preparation, "infinite" (111) terraces are poorly active for the reaction of CO_{ads} electro-oxidation, as already reported in the literature [35].

Once the catalytic behavior of the "quasi-perfect" (111) terrace has been assessed, the next experiment, shown in Figure 3, aims to evaluate the intrinsic catalytic activity of Pt(110)-type steps toward CO electro-oxidation reaction. The intrinsic catalytic activity of step sites means that the activity is evaluated in a condition in which CO_{ads} species are present exclusively on the step sites, being all the (111)-type terraces non-occupied by CO_{ads}. To achieve this situation, a full CO_{ads} layer on a stepped Pt surface was voltammetric electro-

oxidized in a carefully designed experiment. A Pt(776) stepped surface was used as a representative stepped surface. A full CO_{ads} layer was formed on a Pt(776) electrode at a constant potential of 0.1 V. For that, a stream of CO was bubbled through the solution for 5 minutes. After that, non-adsorbed CO in the bulk of the solution was properly eliminated for 30 minutes by bubbling Ar. Then, the CO_{ads} layer was partially oxidized in several voltammetric cycles by carefully controlling the upper potential limit. In order to monitor the extent of vacancies on the top of the CO_{ads} layer on the (111) terrace sites in each voltammetric cycle, the profile of the hydrogen region was registered, and in each subsequent potential cycle, the upper potential limit imposed was progressively increased. Thus, after successive voltammetric cycles, the condition of CO_{ads} species occupying only the (110)-type step sites was achieved. As aforementioned (***Subsection 3.1***), the hydrogen desorption region serves to determine the presence of adsorbed molecules on the different sites, due to the extreme sensitivity of the $H^+ + e^- + {}^*_{\text{active sites}} \rightleftarrows H_{ads}$ reaction to the surface structure. Thus, hydrogen desorption from the (111) terraces gives rise to a wide voltammetric wave in which an almost constant current between 0.06 and 0.18 V is observed, whereas the peak at ~0.13 V corresponds to the desorption of hydrogen from the top of the (110) steps. If any foreign species binds to Pt sites more strongly than H_{ads} does, then the foreign species displaces H_{ads} and occupies the available sites left by the H_{ads} species. Under these conditions, the voltammetric profile in the hydrogen region is due to the hydrogen desorption from the sites not occupied by the foreign species. No other surface technique allows monitoring this type of surface reaction with the detail provided by the voltammetric technique.

Data in Figure 3 (blue line) offer pieces of evidence that when the potential is scanned in a region of high potential, high enough to electro-oxidize a fraction of CO coverage, the set of sites left (available) corresponds to or involves preferentially (111) terrace sites. In this case, a full layer of CO_{ads} was partially oxidized by voltammetry applying different upper potential limits. Generally, successive partial oxidation cycles are necessary in order to remove only CO from the (111) terrace sites of stepped surfaces. The blue line in Figure 3 only shows the last stage of the experiment. As it can be seen, all the (111) terrace sites are available for the $H^+ + e^- + {}^*_{\text{active sites}} \rightleftarrows H_{ads}$ reactions, while only the (110)-type steps (presumably the top of the steps) remains blocked by CO_{ads}. We obtained the condition of CO adsorbed only on the steps because CO electro-oxidation takes place on top of the steps only when all the CO_{ads} on the (111) terraces are electro-oxidized, because the electro-oxidation of CO takes

place preferentially involving (111) terrace sites of defected Pt surfaces. It has been found that this behavior is general for all the surfaces consisting of (111) terraces and (110) steps, in short, for all the stepped surfaces belonging to the Pt(s)-[(n – 1)(111)×(110)] series [39] and is probably related to the higher adsorption energy of CO on the step [40].

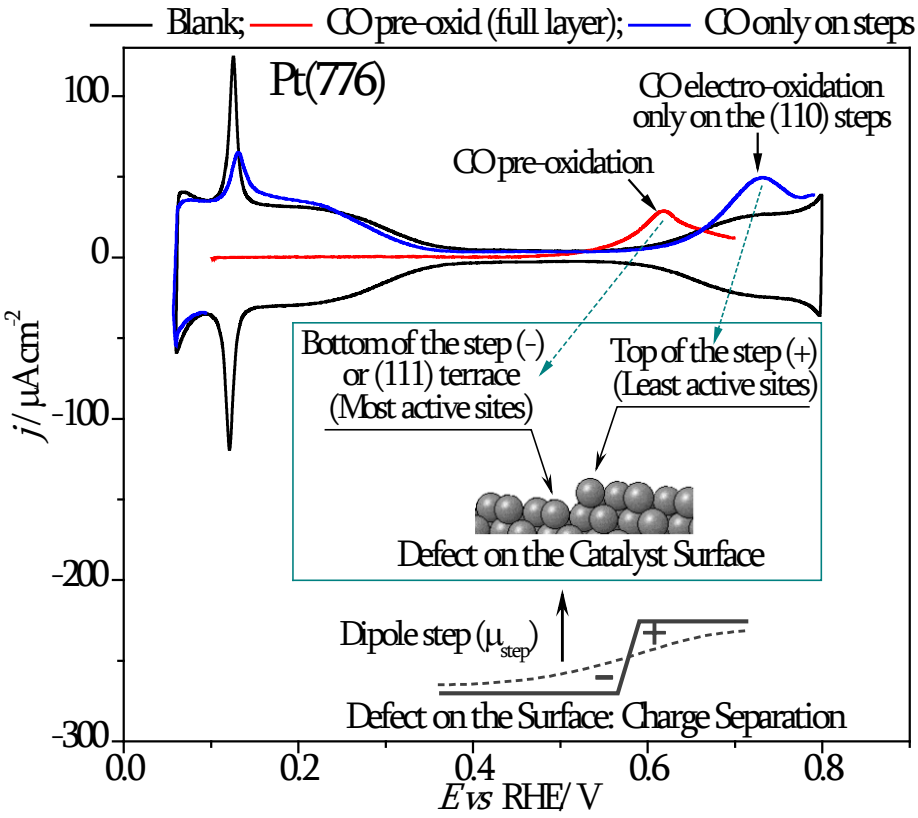

Figure 3. Voltammetric profiles (at 0.05 V s^{-1}) of the electro-oxidation of two different CO_{ads} coverage (full CO_{ads} layer and CO_{ads} only on steps) on a Pt(776) electrode in a 0.1 M $HClO_4$ solution. The CO gas was admitted in the cell with the electrode fixed at 0.1 V. Red line: CO pre-oxidation wave for a full CO_{ads} layer where non-adsorbed CO was removed from solution by bubbling Ar gas for 18 min. Blue line: electro-oxidation of CO_{ads} layer that occupies only the (110)-type steps; the non-adsorbed CO was removed by bubbling Ar gas for 30 min. Black line: cyclic voltammogram obtained in the absence of CO.

In the voltammetric stripping of CO_{ads} only on (110)-type steps (Figure 3, blue line), the peak corresponding to the CO electro-oxidation in these sites appears at ~0.72 V (at a scan rate of 0.05 V s^{-1}). For this type of experiment employing CO_{ads} sub-layer, the *in situ* FTIR spectra showed a single band assigned to the linearly bonded CO on the step sites [7]. Moreover, it was observed that the position of the CO_{ads} band in the *in situ* FTIR spectra is insensitive to the step density, suggesting that inter-molecular coupling is restricted to CO_{ads} species along a line of steps [41]. For comparison, Figure 3 also shows a part of the

voltammetry of electro-oxidation of a full CO_{ads} layer corresponding to the potential range of CO pre-oxidation (showed in the red line). This experiment was extracted from a figure that will be presented later. These two experiments allow a direct comparison between the zones of potentials in which the CO_{ads} oxidation reaction occurs involving exclusively the step (defect) sites and the range of potentials in which the CO pre-oxidation occurs. As it can be seen, the pre-oxidation of CO_{ads} occurs in a range of potentials (significantly) below the range of potentials in which the oxidation of CO_{ads} occurs in the step sites. This comparison is essential for the interpretation of the experiments in the following sections.

3.3. Electro-oxidation of CO on Pt stepped surfaces at different scan sates with traces of CO in solution

Figure 4 presents the experiments of stripping of the CO_{ads} layer on a Pt(776) surface recorded at different scan rates. To register the experiments, the potential was fixed at 0.1 V, and a stream of CO gas was bubbled through the solution for 5 minutes, after which non-adsorbed CO was partially eliminated from the bulk of the solution for 18 minutes. Then, two consecutive cyclic voltammograms were recorded: the CO stripping profile and the subsequent "blank" cyclic voltammogram. As shown in Figure 4A, the voltammograms present two CO electro-oxidation peaks: the main CO electro-oxidation peak (at higher potentials) and a small CO electro-oxidation process at lower potentials, the so-called CO pre-oxidation wave. To better show this region, an enlargement of these pre-oxidation zones of Panel A are shown in Panel B. Since CO was not completely eliminated from the bulk of the solution (only 18 minutes of the purge were deliberately applied), the "blank" cyclic voltammogram of Pt(776), recorded right after the register of CO stripping, always presented a small blockage of sites, which correspond to the (110)-type steps in hydrogen region (see Figure SI 1). This partial site blockage is due to the adsorption of residual CO molecules from the solution, and for that reason, the "blank" cyclic voltammogram also presented a peak potential at ~0.712 V (recorded at a scan rate of 0.02 V s^{-1}), which is due to the electro-oxidation of this CO_{ads} species on the (110)-type steps, as already shown in Figure 3 at another scan rate. Therefore, in Figure 4 the CO stripping on a Pt surface refers to the electro-oxidation of a full CO_{ads} layer formed at 0.1 V and equilibrated with CO traces in the bulk of the solution. In Figure 4, the insets in each panel show the respective slopes obtained from the dependence between the peak potentials and logarithms of the scan rate ($dE_p/d\,logv$)

from respective cyclic voltammograms, which are 83 and 74 mV dec^{-1} for the CO pre-oxidation (Panel A) and main CO electro-oxidation peaks (Panel B), respectively.

To determine the effect of the CO traces on the stripping voltammogram, the experiments in Figure 4 were repeated using a purging time for elimination of the non-adsorbed CO of 10 minutes (Figure 5). Similar to that in Figure 4, voltammograms of CO stripping presented a pre-oxidation process (which is larger than the previous case) and a main CO electro-oxidation peak. The $dE_p/d\,logv$ slopes for CO pre-oxidation (Panel B) and main CO electro-oxidation peak (Panel A) were 54 and 60 mV dec^{-1}, respectively.

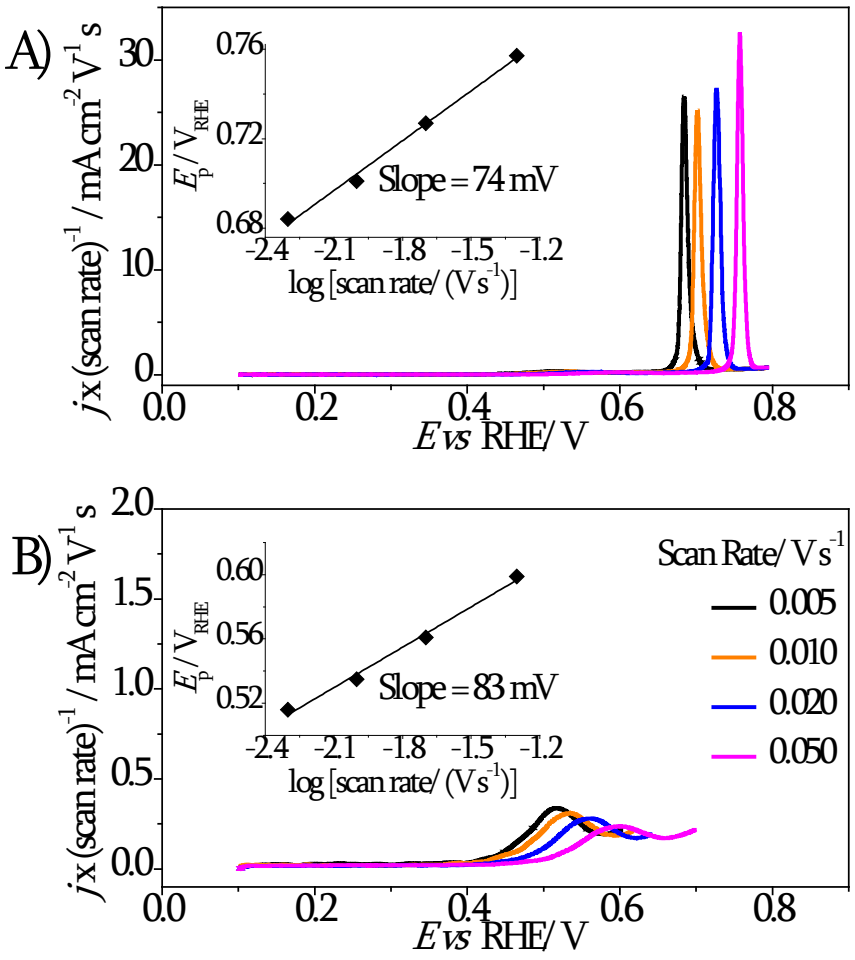

Figure 4. Voltammetric profiles divided by the scan rate of a CO_{ads} layer on a Pt(776) electrode at different scan rates in 0.1 M $HClO_4$. The CO gas was admitted in the cell with the electrode fixed at 0.1 V and non-adsorbed CO was removed for 18 min. A) Main CO oxidation peak. B) Enlargement of the CO pre-oxidation region. Insets: plot of the peak potentials *versus* the logarithm of the sweep rate for the CO pre-oxidation (A) and main CO electro-oxidation peaks (B), recorded respectively from the cyclic voltammograms.

The data in Figures 4 and 5 show that $dE_p/d\,logv$ slopes are strongly influenced by the presence of CO trace in solution. This fact introduces a serious problem to interpret the $dE_p/d\,logv$ slope in terms of the reaction mechanism, so that, at least in the specific case of this work, this parameter seems not suitable for determining the electrochemical reaction mechanism (as the slope is usually used [42]). In fact, due to the complex nature of the CO electro-oxidation process, kinetic modeling shows that different Tafel slopes can be obtained at different potentials for the same reaction mechanism [43].

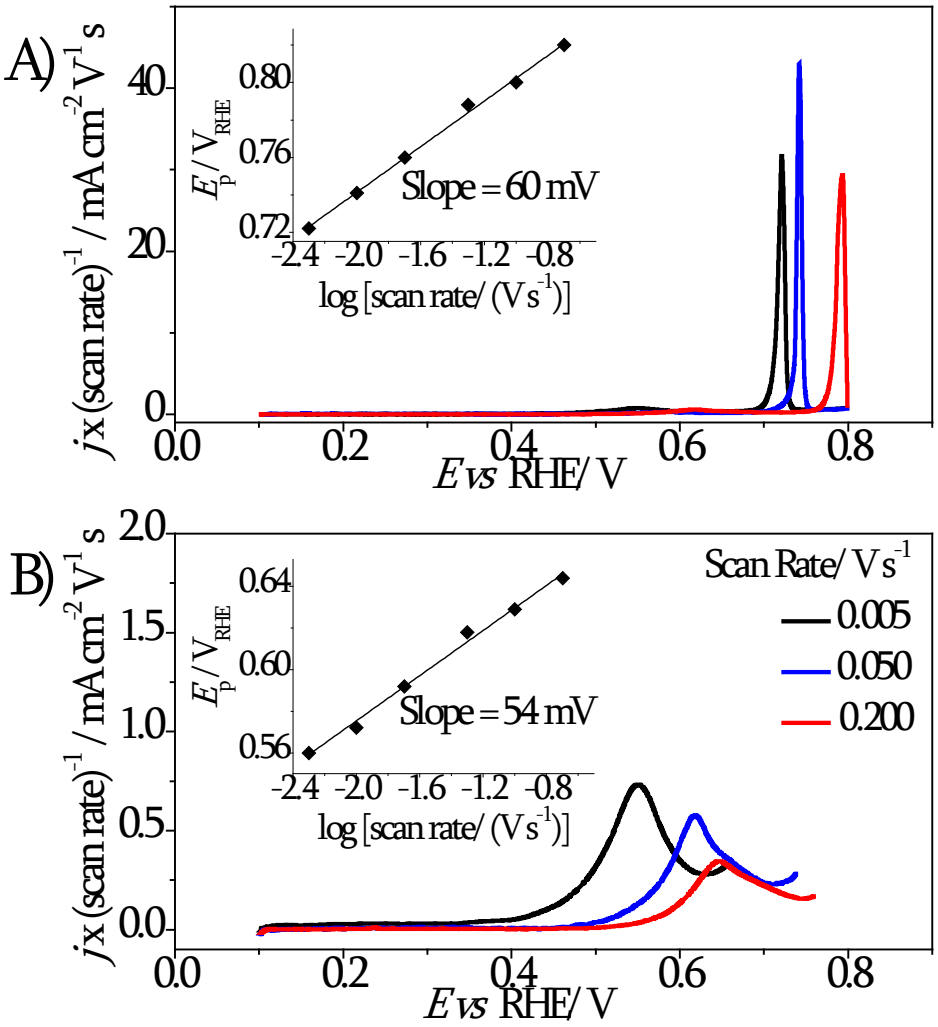

Figure 5. Voltammetric profiles divided by the scan rate of a CO_{ads} layer on a Pt(776) at different scan rates recorded in 0.1 M $HClO_4$ with CO traces. The CO gas was admitted in the cell with the electrode fixed at 0.1 V and non-adsorbed CO was removed from solution by bubbling Ar gas for 10 min. A) Main CO oxidation peak. B) Enlargement of the CO pre-oxidation region. Insets: plot of the peak potentials *versus* the logarithm of the sweep rate for the CO pre-oxidation (A) and main CO electro-oxidation peaks (B), recorded respectively from the cyclic voltammograms.

The magnitude of the charge density of the CO pre-oxidation for CO stripping (after correcting the contribution of the electric double layer [36]) in Figures 4 and 5 were calculated by integration of the curve between 0.4 V (the "onset" potential of CO electro-oxidation) and the potential corresponding to the minimum after the CO pre-oxidation wave of each curve. The charge density values are dependent on the scan rate and purging time. Thus, for 18 minutes of purging time (Figure 4), the charge densities for CO pre-oxidation wave were about 35 and 30 μC cm^{-2} at scan rates of 0.005 and 0.050 V s^{-1}, respectively, whereas, for 10 minutes of purging time (Figure 5), the charge densities of CO pre-oxidation were about 79 and 60 μC cm^{-2}, for the same scan rates, respectively. From these comparative results, it can be seen that: (i) the charge density of CO pre-oxidation tends to be higher when the scan rate is slower; (ii) the magnitude of the CO pre-oxidation is greater for low purging times of non-adsorbed CO elimination. Based on this comparison, it seems that the CO in the bulk of the solution is an important factor that determines the magnitude of the CO pre-oxidation. We are aware that the amount of CO in the bulk of the solution is not an easily controllable parameter. For this reason, we chose to work with large differences (more than 8 minutes) in purging times to eliminate the CO from the bulk of the solution.

Analogously to the experiments employing the Pt(776) electrode, the Pt(13 13 12) electrode was also studied, whose results are shown in Figures 6 and 7 (Panel B in each figure highlight the CO pre-oxidation on an enlarged current scale). Then, on one hand, when non-adsorbed CO was eliminated for 18 minutes of purging time, the $dE_p/d\,logv$ slopes were equal to 66 and 89 mV dec^{-1} for CO pre-oxidation and main CO electro-oxidation peaks, respectively (inset in Figure 6). On the other hand, when non-adsorbed CO was eliminated for 10 minutes only, the $dE_p/d\,logv$ slopes measured 56 and 56 mV dec^{-1} for CO pre-oxidation and main CO electro-oxidation peaks, respectively (inset in Figure 7). As observed for Pt(776) and Pt(13 13 12) electrodes, the presence of CO in the bulk of the solution, even in a small amount, influences the $dE_p/d\,logv$ slopes values, being lower for the solution with higher dissolved CO content. Also, the charge densities of CO pre-oxidation in the two different conditions mentioned above follows the same trend as that described for the Pt(776) electrode. In this sense, when non-adsorbed CO was eliminated from the solution for 18 minutes of purging time, (Figure 6), the charges of CO pre-oxidation were about 46 and 36 μC cm^{-2} for scan rate of 0.010 and 0.050 V s^{-1}, respectively. When non-adsorbed CO was eliminated from the bulk of the solution for only 10 minutes of purging time, (Figure 7), the

charge of CO pre-oxidation was about 71 and 54 μC cm^{-2} for scan rate of 0.010 and 0.050 V s^{-1}, respectively.

The results in Figures 4-7 show that the charge density of the CO pre-oxidation does not depend on the structure of the surface, since the magnitude of the CO pre-oxidation apparently depends on the diffusion of CO from the diffusion layer to the surface sites.

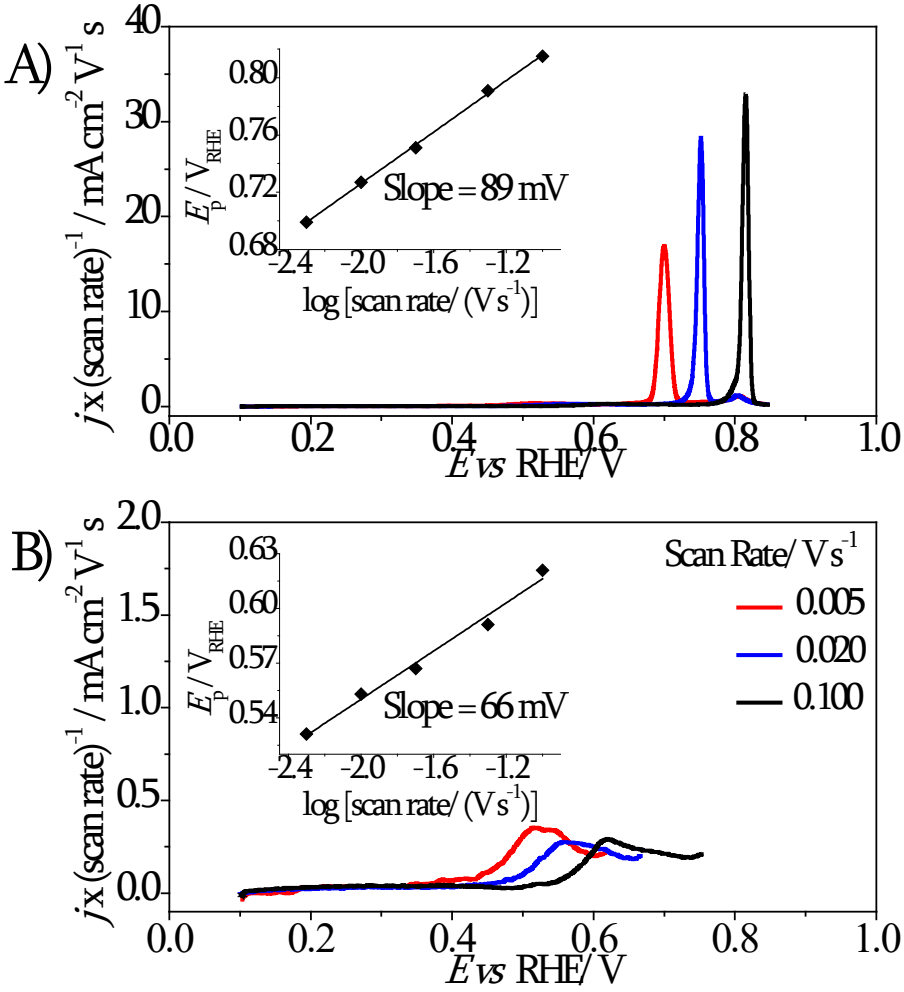

Figure 6. Voltammetric profiles divided by the scan rate of a CO_{ads} layer on a Pt(13 13 12) electrode at different scan rates in 0.1 M $HClO_4$. The CO gas was admitted in the cell with the electrode fixed at 0.1 V and non-adsorbed CO was removed for 18 min. A) Main CO oxidation peak. B) Enlargement of the CO pre-oxidation region. Insets: plot of the peak potentials *versus* the logarithm of the sweep rate for the CO pre-oxidation (A) and main CO electro-oxidation peaks (B), recorded respectively from the cyclic voltammograms.

It should be highlighted that, in Figure 7, the charge density of CO pre-oxidation (~57 μC cm^{-2}) at a scan rate of 0.20 V s^{-1} was slightly higher than the charge density of CO pre-oxidation at 0.05 V s^{-1}. However, the difference falls within the error range of the experiment.

To illustrate this point, Figure 8 shows a series of three different experiments performed in similar experimental conditions: CO was adsorbed at 0.1 V by bubbling CO gas through the solution for 5 minutes (employing the same flow of CO gas) and the non-adsorbed CO was eliminated for 10 minutes (employing the same flow of Ar gas). We chose the Pt(13 13 12) as a representative surface, and CO stripping was recorded at 0.02 V s^{-1}. The results are shown in Figure 8, and the average charge density of CO pre-oxidation ($Q'_{COpre-oxid}$) was 54 ± 4 μC cm^{-2}. It should be noted that after each CO stripping experiment, the electrode was flame annealed so that each experiment was performed with a newly prepared electrode surface. As can be seen in Figure 8, there is a small variation in the charge density of CO pre-oxidation, within acceptable limits.

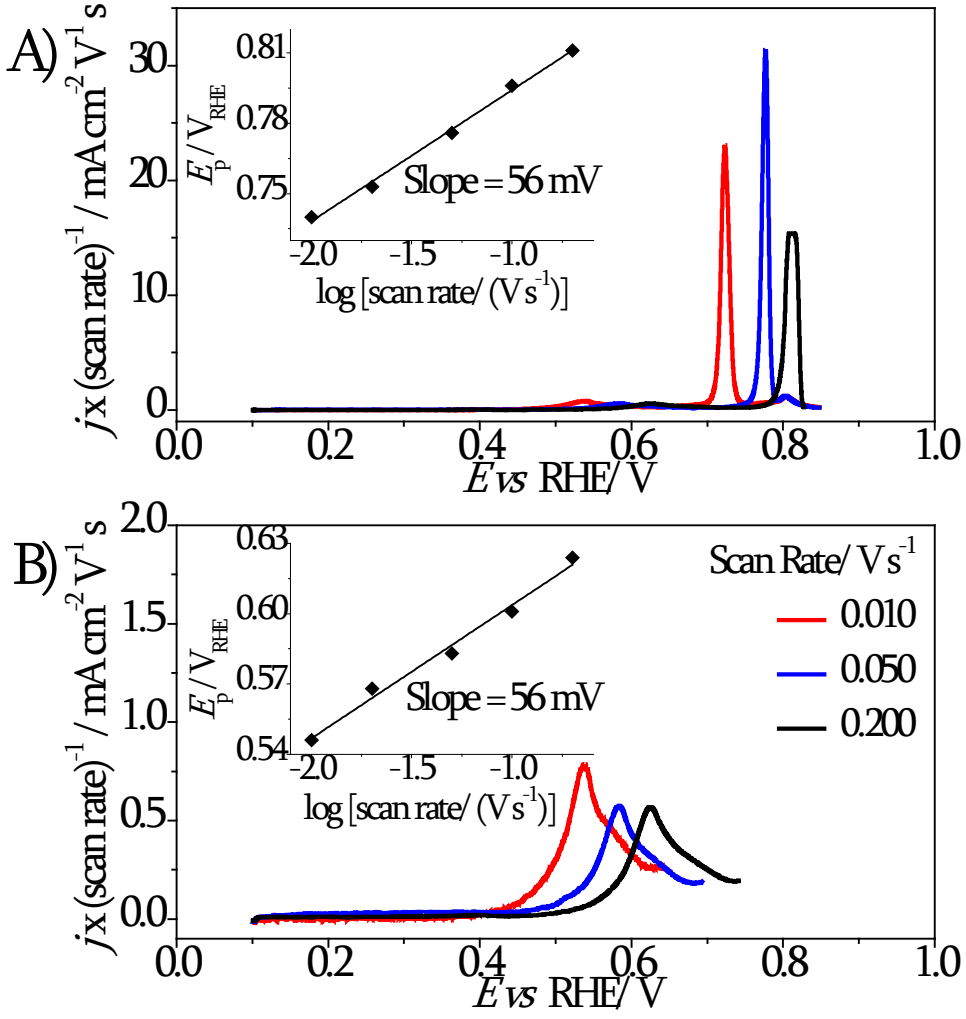

Figure 7. Voltammetric profiles divided by the scan rate of a CO_{ads} layer on a Pt(13 13 12) electrode at different scan rates in 0.1 M $HClO_4$ with CO traces in the solution. The CO gas was admitted in the cell with the electrode fixed at 0.1 V and non-adsorbed CO was removed for 10 min. A) Main CO oxidation peak. B) Enlargement of the CO pre-oxidation region. Insets: plot of the peak potentials *versus* the logarithm of the sweep rate for the CO pre-oxidation (A) and main CO electro-oxidation peaks (B), recorded respectively from the cyclic voltammograms.

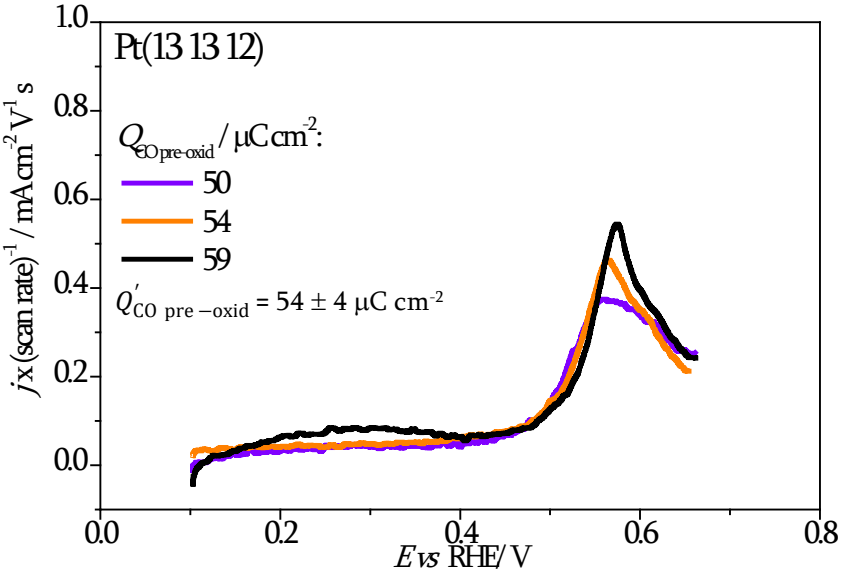

Figure 8. Voltammetric profiles divided by the scan rate of the for three different CO stripping experiments using the same conditions on a Pt(13 13 12) electrode in a 0.1 M $HClO_4$ with CO traces at 0.02 V s^{-1}. The CO gas was admitted in the cell with the electrode fixed at 0.1 V and non-adsorbed CO was removed from solution by bubbling Ar gas for 10 min.

3.4. Effect of the adsorption potential on the CO pre-oxidation in the presence of CO traces in solution

Figure 9 shows the influence of the CO adsorption potential (E_{CO}) on the catalytic activity of the platinum electrodes for the CO electro-oxidation. Five different potentials for the CO adsorption were considered. To register these experiments, a stream of CO gas was bubbled through the solution for 5 minutes, and non-adsorbed CO was eliminated for 10 minutes. In Figure 9, Panel B shows the data on Panel A on a scale to enlarge the CO pre-oxidation zone. As it can be seen, the adsorption potential is a critical factor determining the magnitude of the CO pre-oxidation wave. In addition, the total CO coverage was calculated and the results were as follows: for adsorption potential of 0.06, 0.10, 0.20, 0.25, and 0.35 V, the total CO coverage (θ_{CO}) were about 0.73, 0.71, 0.71, 0.69 and 0.67, respectively. The CO pre-oxidation was the highest for CO adsorption potential of 0.06 V and did not appears for CO adsorption potentials higher than ~0.25 V. Two experiments with CO saturated solutions were also performed, shown in Figure 9, and two CO adsorption potentials were considered, namely, 0.10 and 0.35 V. In this case, CO gas was admitted into the electrochemical cell (by bubbling CO gas for 5 minutes) and non-adsorbed CO was not eliminated from the bulk of the (quiescent) solution (experiments shown in Figure 9 in the black and olive lines for CO

adsorption and 0.10 and 0.35 V, respectively). As it can be observed, for the CO saturated solution, the CO oxidation reaction starts at very low overpotentials and the current density (due to the CO electro-oxidation) is very high, indicating a fast reaction. Moreover, unlike CO stripping shown in gray line, even when the CO adsorption potential was about 0.35 V for the CO saturated solution (Figure 9, olive line), the CO electro-oxidation reaction starts at very low overpotentials, or rather, at the potential zone of the CO pre-oxidation. Based on the set of experiments displayed in Figure 9, CO in the bulk of the solution is a necessary condition for the oxidation of CO at low overpotentials. Finally, it is important to highlight that the peak potential of CO pre-oxidation (and the main oxidation peak as well) shifts to more positive potentials as the potential of adsorption of CO gets more positive. Employing a randomly defected Pt(111)-type electrode, López-Cudero *et al.* [14] observed a similar effect of CO adsorption potential on CO pre-oxidation.

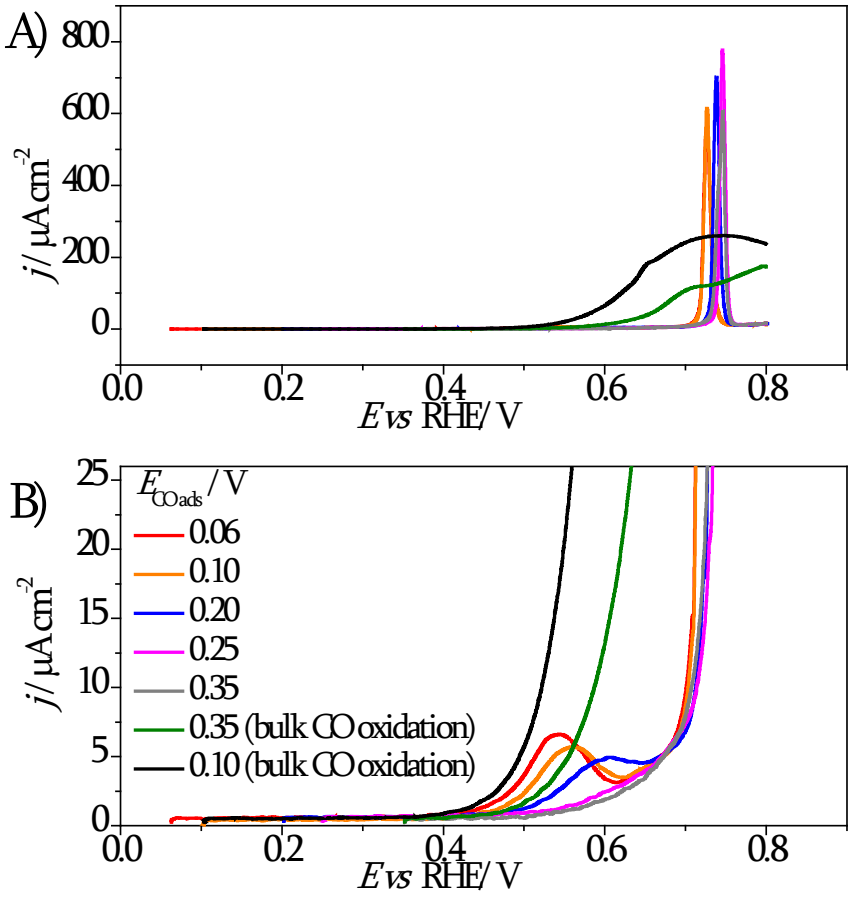

Figure 9. Effect of CO adsorption potential on the ignition potential for CO electro-oxidation on a Pt(776) electrode in 0.1 M $HClO_4$ at 0.02 V s^{-1}. The CO gas was admitted at different potentials (shown in the figure) and non-adsorbed CO was removed from the solution by bubbling Ar gas for 10 min. For comparison, two experiments with a CO saturated solution are also presented. A) Enlargement of the CO pre-oxidation region. B) Main CO oxidation peak: CO adsorption at 0.10 V (black line); CO adsorption at 0.35 V (olive line).

4. Discussion

The discussions are centered on two main findings: (i) defects on the catalyst surface do not behave as active sites in the potential region where the CO pre-oxidation appears; (ii) CO pre-oxidation involves the diffusion-limited process of bulk CO electro-oxidation.

4.1. Catalytic activity of defect sites and the most active sites

For the electro-oxidation reaction of CO, the most reliable way to measure the catalytic activity of surface Pt defect sites consists of selectively marking (or decorating) these sites with CO_{ads} while maintaining the potential in a region where CO_{ads} does not oxidize to CO_2, and then increasing the potential to values where it does oxidize. In this case, it is possible to register the electric current generated from the electro-oxidation of CO, or in more sophisticated cases, the formation of CO_2 can be monitored by using a suitable molecular probe such as vibrational spectroscopy (*in situ* FTIR) [29]. The experiments in Figure 3 follow the first option and provide pieces of evidence that the top of the defects on the surface can be considered as inactive sites for the CO electro-oxidation in the region of potentials in which the pre-oxidation process takes place. Quantitatively comparing experiments at the same scan rate and similar platinum surface, the CO pre-oxidation visibly starts at potentials around 0.46 V (Figure 3, red line), whereas the electro-oxidation of CO_{ads} on top of the step sites only starts at potentials around 0.66 V (Figure 3, blue line). Logically, the CO pre-oxidation takes place involving the set of most active sites. On Pt(111) terraced surfaces, the most active sites are located on the bottom of (111) terraces, as previously proposed for a study involving CO pre-oxidation on platinum in acid media [7]. Then, there is a wide potential difference of about 200 mV (or 0.66 V_{RHE} – 0.46 V_{RHE} = 0.20 V) separating the onset potential of the CO electro-oxidation involving the set of most active sites and the onset potential of electro-oxidation of CO on the sites at the top of the steps. With regard to that, interestingly, like a contrasting effect, the potential difference between the most active sites and the rest increases with increasing pH of the solution [39]. For example, in an alkaline solution (pH around 13), the difference of onset potential involving these sites, that is, most active sites and top of the steps of stepped Pt surfaces, reaches about 0.4 V (as inferred from the data in Figure 12 in this reference [44]). In general, defects on the surface can tune the catalytic properties that emerge on the (111) terraces of these surfaces, with such catalytic properties absent on "infinite" (111) terraces [23].

4.2. Role of CO in the bulk of the solution on the CO pre-oxidation

To evaluate the influence of the CO concentration in the bulk of the solution on the magnitude (and the shape of the curve) of the CO pre-oxidation, it should be taken into consideration that only the set of most active sites work at potentials of the CO pre-oxidation wave, while all the top of the defect sites are entirely inactive (or poisoned by CO_{ads}) at that potentials. In this sense, the defects on the surface do not directly contribute as active sites to the CO pre-oxidation charge density (**Subsection 4.1**). Then, if dissolved CO is present in the solution, a portion of most active sites released during CO pre-oxidation can be re-occupied again with CO diffusing from the bulk of the solution (diffusion layer), and then CO molecules might be "continuously" electro-oxidized on these sites. What suggest that, the scan rate should have an impact on the pre-oxidation wave. This seems a reasonable hypothesis because, at first glance, the CO pre-oxidation resembles a "continuous" process of CO electro-oxidation, as it will be analyzed in detail below. It is important to note that we are discussing the pre-oxidation of CO when it appears under very specific conditions applied in the preparation of the CO_{ads} layer on a certain type of catalytic surface, since the pre-oxidation can be originated by different factors (even on the same type of surface and electrolyte) [23]. If this hypothesis about re-occupation of sites released during the CO pre-oxidation by CO from the solution is correct, two consequences must be expected: (1) the charge density of CO pre-oxidation wave must be higher for slower scan rates; and (2) the charge of CO pre-oxidation must increase with the increase of the CO concentration in the bulk of the solution. The measured charge densities of CO pre-oxidation presented in **Subsection 3.3** corroborate those two expected consequences described in (1) and (2) above.

The CO concentration in solution has a third consequence: it alters the slope of the potential of peaks of CO pre-oxidation versus the logarithm of scan rate, *i.e.*, $dE_p/d\,logv$. This slope diminishes when the bulk CO increases (Figures 4-7). Unfortunately, the interpretation of this change is not straightforward. The change in Tafel slopes is often assumed to reflect the change in the rate-determining step of an electrochemical reaction, in this specific case, the electro-oxidation of CO. However, the electro-oxidation reaction of CO involves the transfer of two electrons and two protons, and for this reason, the reaction proceeds through a series of elementary electrochemical (and possible chemical) steps and

involving many adsorbed reaction intermediates. In this line, spectroscopic results (by *in situ* electrochemical SHINERS) have recently shown that the CO electro-oxidation on Pt(111) proceeds via the formation of adsorbed COOH [45]. When adsorbed species are involved, the adsorption isotherms affect the Tafel slope, so that changes in the Tafel slope can be observed without a change in the oxidation mechanism [43]. In fact, when adsorbed species are involved in reaction mechanisms, the Tafel slope is only constant in the very low coverage regime. Thus, the change in the slope only reflects the changes in the coverage of the species involved in the pre-oxidation wave, which is the result of the diffusion of bulk CO (diffusion layer) to most active sites on the Pt surface released during the CO pre-oxidation. In this regard, data in this paper suggest that, in a quiescent solution containing CO *at level traces*, the rate of CO electro-oxidation reaction is higher than the rate of provision of CO molecules via diffusion to Pt active sites released during the CO pre-oxidation. The basis for this statement is that the content of CO (at trace level) in the bulk of the quiescent solution strongly determines the magnitude (and the shape of the curve) of the CO pre-oxidation feature [7], as a diffusion limitation process.

The argument presented above is qualitative, but it can be expressed in more quantitative terms when the CO bulk concentration is considered. For irreversible processes controlled by diffusion, the Randles-Ševčík equation (equation 1) [46] can be applied to calculate the peak current intensity (i_p).

$$i_p = 2.6910^5 n^{3/2} A D_0^{1/2} c_0 v^{1/2} \qquad (1)$$

In this equation, n is the number of electrons that cross the electrochemical interface per molecule of electro-oxidized CO; A is the electrode surface area, specifically, oriented area of the Pt crystal in contact with the solution; D_0 is the diffusion coefficient of the CO in the solution whose bulk concentration is c_0; v is the potential scan rate. Data obtained from Figures 4-7, applying equation 1, are presented in Figure 10. For each curve in Figure 10, all the parameters except v are constant and thus the plot of i_p versus $\sqrt{v}$ should be linear for processes controlled by diffusion. As it can be seen, a linear behavior is obtained, corroborating the involvement of diffusion in the pre-oxidation regime. Since the term $n^{3/2} A D_0^{1/2}$ is constant for the whole set of experiments, the change in slope between the different experiments reflects the change of bulk CO concentration in the different experiments. It should be noted that, for different surfaces, the different sets of experiments with the same purging time have the same slope within the error of the measurements,

highlighting the reproducibility of the experimental method employed. For two series of experiments with the Pt(13 13 12) electrode and considering 10 and 18 minutes of purging time for non-adsorbed CO elimination, the slopes were ~7.7 and ~2.2 $\mu A \cdot V^{-1/2} \cdot s^{1/2}$, respectively (Figure 10). These results indicate that the concentration in the solution for 10 min purging time is about 3.5 times higher than that degassed for 18 minutes.

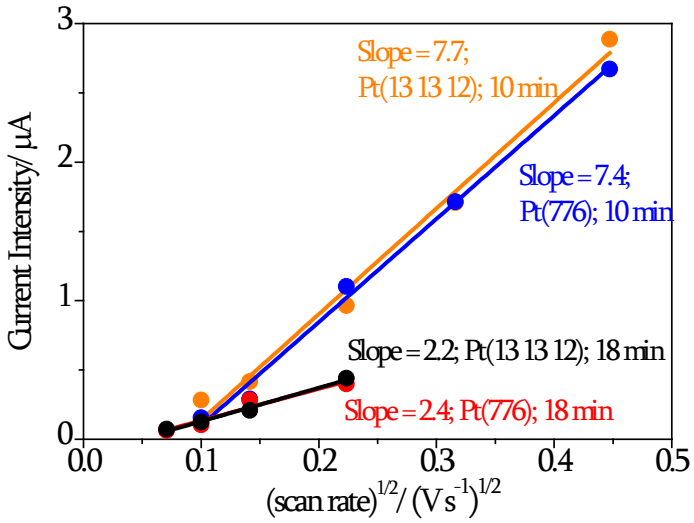

Figure 10. Plot of peak current densities of the CO pre-oxidation wave vs. the square root of the scan rate on the Pt(13 13 12) and Pt(776) electrodes, using two different times for elimination of non-adsorbed CO from the solution (shown in the figure). Data obtained from Figures 4-7.

This unambiguously proves that the intensity and the shape of the curve of the CO pre-oxidation depends on the content of CO in the solution, when at the trace level. However, it is necessary to bring some light to other assumptions implicit in the statement above. One of these implicit assumptions is that in the CO electro-oxidation reaction, the concentration of the species that act as the external oxygen source is constant in CO pre-oxidation feature. This means that for the formal reaction $CO_{ads} + (H_2O)_{activated} \rightleftarrows CO_{2(g)} + 2H^+ + 2e^-$, the concentration of $(H_2O)_{activated}$ water-type is constant. This argument seems reasonable, at least when the same CO adsorption potential is considered since the peak potential for the CO pre-oxidation is affected by the potential of CO dosing (Figure 9). Therefore, the argument presented here is that during the CO pre-oxidation, there is a quasi-continuous electro-oxidation which involves CO molecules coming from the bulk of the solution to occupy the most active sites continuously released during the CO pre-oxidation. It is important to highlight that the most active sites released during the CO pre-oxidation are not re-occupied by CO_{ads} from any other sites, that is, there is no re-occupation of the most active sites

involving CO surface diffusion. This subject will be discussed later. A look at Figure 9 (black and olive traces) indicates that for a quiescent solution saturated with CO, the reaction of CO electro-oxidation is very fast in the range of CO pre-oxidation potentials and the CO molecules are being continuously oxidized in a reaction limited to these very active sites. Thus, the oxidation rate in this pre-oxidation region depends on the number of very active sites and the diffusion rate. The data of Figure 9 for CO adsorbed at 0.10 V corroborate this proposition. When the non-adsorbed CO is eliminated from solution by bubbling Ar gas for 10 min (orange trace), the peak current density is ~5.7 μA cm^{-2} at 0.56 V; on the other hand, for the solution saturated with CO, the current density at that potential is ~26 μA cm^{-2}. Then, for CO saturated solution, the reaction speed is about 4.6 faster at that potential. For CO saturated solution, since the bulk CO concentration is more than 4.6 times that obtained when the solution is purged for 10 min, all molecules that reach the *most active sites* are promptly electro-oxidized under this trace CO concentration. Evidently, when forced convection (as in rotating disk electrode configuration) is used, the CO pre-oxidation is hindered and occurs simultaneously with the electro-oxidation of CO from the solution [24]. Therefore, since CO in solution determines the magnitude and the shape of the curve of the CO pre-oxidation, the role of the CO in solution might confluence to at least two complementary effects: (*i*) quick provision of CO molecules to the most active sites released during the CO pre-oxidation; (*ii*) ensure high local CO coverage involving the most active sites, rather, the active center.

In principle, knowing the electrode surface area (A) and the diffusion coefficient (D_0) of the species that determine the peak current intensity for the oxidation and applying the Randles-Ševčík equation, the concentration of CO in the solution can be determined from the slope i_p versus $\sqrt{v}$. In this case, on one hand, the CO pre-oxidation process also involves, possibly a significant ratio, the electro-oxidation of CO molecules that are already on the electrode surface and consequently a fraction of the current at the peak potential i_p is originated from electro-oxidation of CO molecules that are not diffusing from the solution. For this reason, the Randles-Ševčík equation is not fully applicable to this situation and concentrations cannot be determined. However, the observed linear response when i_p is plotted *vs* $\sqrt{v}$ is still an indication that diffusion of CO from the diffusion layer to the surface sites is the main contribution to this process. On the other hand, the main CO electro-oxidation process is dominated by the electro-oxidation of CO_{ads} species that are already on the electrode surface. For this reason, as Figure 4 shows, the peak pseudo-capacitance is

independent of the scan rate, which implies that the peak current density is directly proportional to the scan rate. This is the typical behavior of a surface-confined process. These differences can be rationalized using the following arguments. The time span (Δt) during which the CO pre-oxidation occurs is much longer than the one for the electro-oxidation of CO in the main process. Let us consider the experiments carried out at the scan rate of 0.02 V s^{-1}. The potential window that comprises the CO pre-oxidation process is ~0.21 V (where Δt ~ 10 s) whereas the potential window for the main process is narrower, about 0.12 V (where Δt ~ 6 s), see, for example, data in Figure 5. The charge involved in the main CO electro-oxidation process (about 270 μC cm^{-2}) is significantly higher than the CO pre-oxidation one (ranges from ~30 to ~80 μC cm^{-2}, depending on the purging time for elimination of the non-adsorbed CO). Then, when a quiescent solution contains CO at level traces, the charge that crosses the interface due to the electro-oxidation of CO molecules diffusing from the bulk of the solution to the previously released Pt sites is negligible in comparison to the charge density of a CO_{ads} layer corresponding to the main CO electro-oxidation process. Therefore, conceptually, the CO pre-oxidation involves the diffusion-limited electro-oxidation of bulk CO, while the main CO electro-oxidation peak is typical of a surface-confined process.

Now we are going to make some considerations about the diffusion of CO on surface during the electro-oxidation of the CO_{ads} layer. Another way to interpret the influence of potential scan rate on the charge of CO pre-oxidation is to consider the limited surface diffusion of CO_{ads} from any site on which this species is adsorbed to the reactive sites, as suggested for the electro-oxidation of CO_{ads} on Pt(100) electrode (in principle with the CO-free solution) [18]. For the Pt(111) surface in CO saturated solution at potentials in the pre-oxidation zone, by *in situ* high-speed scanning tunneling microscopy technique, diffusion of CO on surface (from any site to the reactive sites) is assigned to dynamics of defects in the CO_{ads} compressed layer [22]. The dynamics of defects in the CO_{ads} compact layer, when there is CO in the solution, is a very interesting finding. In this regards, in presence of CO containing solution, at potentials below the onset of CO electro-oxidation, the CO_{ads} species in the compressed layer are continuously exchanged by CO from the solution [47]. With respect to surface diffusion of CO_{ads} mentioned above, the point is that, on stepped Pt surfaces, on one hand, the adsorption sites on the terraces have an intrinsic energy gradient being the top of the steps the sites on which CO binds more strongly [40]. On the other hand, on Pt electrodes, CO_{ads} molecules oxidize first in the places where the CO adsorption is weaker [44].

It is not expected that CO_{ads} diffuses over the surface to occupy the most active sites released during the CO pre-oxidation process (at least on the time scale of the experiments). In the "absence" of CO in the solution, a series of experiments employing different electrode materials in different laboratories worldwide [7, 48-50] has shown that once the pre-oxidation is removed, the remaining CO_{ads} species oxidize requiring even higher potentials, suggesting that there is no re-occupation of sites that require surface diffusion as a principle. What appears to be clear for the pre-oxidation region is not directly extrapolatable to the main oxidation process. Therefore, the question of whether CO_{ads} are mobile during its electro-oxidation, that is, wheter CO_{ads} diffuses during its electro-oxidation from less active sites to more active sites remains a major challenge to better understand this reaction.

5. Main Conclusions

In this paper, the main conclusions can be summarized as follows:

i. The CO pre-oxidation takes place at a potential range in which all the (110)-type step sites (top side of defects) are inactive for the electro-oxidation of CO_{ads}. The most active sites, presumable the bottom (111) terraces, initiate the CO pre-oxidation at potentials about 0.20 V lower than those in which the reaction takes place on the (110)-type steps.

ii. The CO traces in the bulk of the solution determines the magnitude and the shape of the curve of the CO pre-oxidation. The role of CO in the bulk of the solution confluences to two complementary effects: (1) quick provision of CO molecules from the bulk of the solution (diffusion layer) to the active sites continuously released during the CO pre-oxidation; (2) ensure high local CO coverage involving the most active sites, rather, the active centers.

iii. Therefore, in presence of CO in the bulk of the solution, the pre-oxidation of CO proceeds involving the diffusion-limited electro-oxidation of bulk CO at most active sites left available during the CO pre-oxidation. The electro-oxidation of CO in the main peak is a typical behavior of a surface-confined process. Conceptually, at least on Pt electrodes in acid media, the experiments evidence that the bulk CO electro-oxidation and the pre-oxidation of CO are connected.

Acknowledgments

Manuel J.S. Farias is grateful to CAPES (Brazil), Financial support from Ministerio de Ciencia e Innovación (Spain) (Project no. PID2019-105653GB-100 and FJC2018-038607-I) and Generalitat Valenciana (Spain) (Project PROMETEO/2020/063).

References

[1] N.M. Marković, P.N. Ross, Surface science studies of model fuel cell electrocatalysts, Surf. Sci. Rep., 45 (2002) 117-229.

[2] M.T.M. Koper, S.C.S. Lai, E. Herrero, Mechanisms of the oxidation of carbon monoxide and small organic molecules at metal electrodes, In: Fuel Cell Catalysis, John Wiley & Sons, Inc., 2008, pp. 159-207.

[3] Lide, D. L. CRC Handbook of Chemistry and Physics, 87th ed.; CRC Press: Boca Raton, FL, 2006–2007.

[4] N.P. Lebedeva, M.T.M. Koper, J.M. Feliu, R.A. van Santen, Mechanism and kinetics of the electrochemical CO adlayer oxidation on Pt(111), J. Electroanal. Chem., 524 (2002) 242-251.

[5] B. Andreaus, F. Maillard, J. Kocylo, E.R. Savinova, M. Eikerling, Kinetic modeling of CO_{ad} monolayer oxidation on carbon-supported platinum nanoparticles, J. Phys. Chem. B, 110 (2006) 21028-21040.

[6] P. Inkaew, C. Korzeniewski, Kinetic studies of adsorbed CO electrochemical oxidation on Pt(335) at full and sub-saturation coverages, Phys. Chem. Chem. Phys., 10 (2008) 3655-3661.

[7] M.J.S. Farias, G.A. Camara, J.M. Feliu, Understanding the CO preoxidation and the intrinsic catalytic activity of step sites in stepped Pt surfaces in acidic medium, J. Phys. Chem. C, 119 (2015) 20272-20282.

[8] E.P.M. Leiva, E. Santos, T. Iwasita, The effect of adsorbed carbon monoxide on hydrogen adsorption and hydrogen evolution on platinum, J. Electroanal. Chem., 215 (1986) 357-367.

[9] K. Kunimatsu, H. Seki, W.G. Golden, J.G. Gordon, M.R. Philpott, Carbon monoxide adsorption on a platinum electrode studied by polarization-modulated FT-IR reflection-absorption spectroscopy: II. Carbon monoxide adsorbed at a potential in the hydrogen region and its oxidation in acids, Langmuir, 2 (1986) 464-468.

[10] H. Kita, K. Shimazu, K. Kunimatsu, Electrochemical oxidation of CO on Pt in acidic and alkaline solutions: Part I. voltammetric study on the adsorbed species and effects of aging and Sn(IV) pretreatment, J. Electroanal. Chem., 241 (1988) 163-179.

[11] H. Kita, H. Naohara, T. Nakato, S. Taguchi, A. Aramata, Effects of adsorbed CO on hydrogen ionization and CO oxidation reactions at Pt single-crystal electrodes in acidic solution, J. Electroanal. Chem., 386 (1995) 197-206.

[12] E. Grantscharova-Anderson, A.B. Anderson, The prewave in CO oxidation over roughened and Sn alloyed Pt surfaces: possible structure and electronic causes, Electrochim. Acta, 44 (1999) 4543-4550.

[13] N.M. Marković, B.N. Grgur, C.A. Lucas, P.N. Ross, Electrooxidation of CO and H_2/CO mixtures on Pt(111) in acid solutions, J. Phys. Chem. B, 103 (1999) 487-495.

[14] A. López-Cudero, A. Cuesta, C. Gutiérrez, Potential dependence of the saturation CO coverage of Pt electrodes: The origin of the pre-peak in CO-stripping voltammograms. Part 1: Pt(111), J. Electroanal. Chem., 579 (2005) 1-12.

[15] C. Jung, J. Kim, C.K. Rhee, Electrochemical scanning tunneling microscopic observation of the preoxidation process of CO on Pt(111) electrode surface, Langmuir, 23 (2007) 9495-9500.

[16] K. Kunimatsu, T. Sato, H. Uchida, M. Watanabe, Role of terrace/step edge sites in CO adsorption/oxidation on a polycrystalline Pt electrode studied by in situ ATR-FTIR method, Electrochim. Acta, 53 (2008) 6104-6110.

[17] G. Samjeské, K.I. Komatsu, M. Osawa, Dynamics of CO oxidation on a polycrystalline platinum electrode: A time-resolved infrared study, J. Phys. Chem. C, 113 (2009) 10222-10228.

[18] A. Cuesta, The oxidation of adsorbed CO on Pt(100) electrodes in the pre-peak region, Electrocatal., 1 (2010) 7-18.
[19] Y.G. Yan, Y.Y. Yang, B. Peng, S. Malkhandi, A. Bund, U. Stimming, W.B. Cai, Study of CO oxidation on polycrystalline Pt electrodes in acidic solution by ATR-SEIRAS, J. Phys. Chem. C, 115 (2011) 16378-16388.
[20] A.V. Rudnev, A. Kuzume, Y. Fu, T. Wandlowski, CO oxidation on Pt(100): New insights based on combined voltammetric, microscopic and spectroscopic experiments, Electrochim. Acta, 133 (2014) 132-145.
[21] H. Wang, H.D. Abruña, Origin of multiple peaks in the potentiodynamic oxidation of CO adlayers on Pt and Ru-modified Pt electrodes, J. Phys. Chem. Lett., 6 (2015) 1899-1906.
[22] J. Wei, R. Amirbeigiarab, Y.-X. Chen, S. Sakong, A. Gross, O.M. Magnussen, The dynamic nature of CO adlayers on Pt(111) electrodes, Angew. Chem. Int. Ed., 59 (2020) 6182-6186.
[23] M.J.S. Farias, A.L.P. Silva, A.A. Tanaka, E. Herrero, J.M. Feliu, Surface defects as ingredients that can improve or inhibit the pathways for CO oxidation at low overpotentials using Pt(111)-type catalysts, J. Phys. Chem. C, 124 (2020) 26583-26595.
[24] C.A. Angelucci, E. Herrero, J.M. Feliu, Bulk CO oxidation on platinum electrodes vicinal to the Pt(111) surface, J. Solid State Electrochem., 11 (2007) 1531-1539.
[25] M.T.M. Koper, T.J. Schmidt, N.M. Marković, P.N. Ross, Potential oscillations and S-shaped polarization curve in the continuous electro-oxidation of CO on platinum single-crystal electrodes, J. Phys. Chem. B, 105 (2001) 8381-8386.
[26] E.A. Batista, T. Iwasita, W. Vielstich, Mechanism of stationary bulk CO oxidation on Pt(111) electrodes, J. Phys. Chem. B, 108 (2004) 14216-14222.
[27] J. Inukai, D.A. Tryk, T. Abe, M. Wakisaka, H. Uchida, M. Watanabe, Direct STM elucidation of the effects of atomic-level structure on Pt(111) electrodes for dissolved CO oxidation, J. Am. Chem. Soc., 135 (2013) 1476-1490.
[28] N.P. Lebedeva, M.T.M. Koper, J.M. Feliu, R.A. Van Santen, Role of crystalline defects in electrocatalysis: Mechanism and kinetics of CO adlayer oxidation on stepped platinum electrodes, J. Phys. Chem. B, 106 (2002) 12938-12947.
[29] M.J.S. Farias, W. Cheuquepán, A.A. Tanaka, J.M. Feliu, Identity of the most and least active sites for activation of the pathways for CO_2 formation from the electro-oxidation of methanol and ethanol on platinum, ACS Catal., 10 (2020) 543-555.
[30] B. Lang, R.W. Joyner, G.A. Somorjai, Low energy electron diffraction studies of high index crystal surfaces of platinum, Surf. Sci., 30 (1972) 440-453.
[31] J. Clavilier, D. Armand, S.G. Sun, M. Petit, Electrochemical adsorption behaviour of platinum stepped surfaces in sulphuric acid solutions, J. Electroanal. Chem., 205 (1986) 267-277.
[32] R. Gómez, V. Climent, J.M. Feliu, M.J. Weaver, Dependence of the potential of zero charge of stepped platinum (111) electrodes on the oriented step-edge density: electrochemical implications and comparison with work function behavior, J. Phys. Chem. B, 104 (2000) 597-605.
[33] A. Berná, V. Climent, J.M. Feliu, New understanding of the nature of OH adsorption on Pt(111) electrodes, Electrochem. Commun., 9 (2007) 2789-2794.
[34] J. Clavilier, K. El Achi, A. Rodes, In situ probing of step and terrace sites on Pt(S)-[n(111) × (111)] electrodes, Chem. Phys., 141 (1990) 1-14.
[35] N.P. Lebedeva, M.T.M. Koper, E. Herrero, J.M. Feliu, R.A. Van Santen, Cooxidation on stepped Pt[n(111)×(111)] electrodes, J. Electroanal. Chem., 487 (2000) 37-44.
[36] R. Gómez, J.M. Feliu, A. Aldaz, M.J. Weaver, Validity of double-layer charge-corrected voltammetry for assaying carbon monoxide coverages on ordered transition metals:

Comparisons with adlayer structures in electrochemical and ultrahigh vacuum environments, Surf. Sci., 410 (1998) 48-61.
[37] A. Cuesta, M.D.C. Pérez, A. Rincón, C. Gutiérrez, Adsorption isotherm of CO on Pt(111) electrodes, ChemPhysChem, 7 (2006) 2346-2351.
[38] I. Villegas, M.J. Weaver, Carbon monoxide adlayer structures on platinum (111) electrodes: A synergy between in-situ scanning tunneling microscopy and infrared spectroscopy, J. Chem. Phys., 101 (1994) 1648-1660.
[39] M.J.S. Farias, G.A.B. Mello, A.A. Tanaka, J.M. Feliu, Site-specific catalytic activity of model platinum surfaces in different electrolytic environments as monitored by the CO oxidation reaction, J. Catal., 345 (2017) 216-227.
[40] C. Busó-Rogero, E. Herrero, J. Bandlow, A. Comas-Vives, T. Jacob, CO oxidation on stepped-Pt(111) under electrochemical conditions: Insights from theory and experiment, Phys. Chem. Chem. Phys., 15 (2013) 18671-18677.
[41] M.J.S. Farias, C. Busó-Rogero, A.A. Tanaka, E. Herrero, J.M. Feliu, Monitoring of CO binding sites on stepped pt single crystal electrodes in alkaline solutions by in situ FTIR spectroscopy, Langmuir, 36 (2020) 704-714.
[42] O.V. Cherstiouk, P.A. Simonov, V.I. Zaikovskii, E.R. Savinova, CO monolayer oxidation at Pt nanoparticles supported on glassy carbon electrodes, J. Electroanal. Chem., 554-555 (2003) 241-251.
[43] C.A. Angelucci, E. Herrero, J.M. Feliu, Modeling CO oxidation on Pt(111) electrodes, J. Phys. Chem. C, 114 (2010) 14154-14163.
[44] M.J.S. Farias, E. Herrero, J.M. Feliu, Site selectivity for CO adsorption and stripping on stepped and kinked platinum surfaces in alkaline medium, J. Phys. Chem. C, 117 (2013) 2903-2913.
[45] M. Su, J.-C. Dong, J.-B. Le, Y. Zhao, W.-M. Yang, Z.-L. Yang, G. Attard, G.-K. Liu, J. Cheng, Y.-M. Wei, Z.-Q. Tian, J.-F. Li, In situ Raman study of CO electrooxidation on Pt(hkl) single-crystal surfaces in acidic solution, Angew. Chem. Int. Ed., 59 (2020) 23554-23558.
[46] J.B. Allen, R.F. Larry, Electrochemical methods fundamentals and applications, John Wiley & Sons, 2001.
[47] M. Heinen, Y.-X. Chen, Z. Jusys, R.J. Behm, Room temperature CO_{ad} desorption/exchange kinetics on Pt electrodes - a combined in situ IR and mass spectrometry study, ChemPhysChem, 8 (2007) 2484-2489.
[48] Y. Morimoto, E.B. Yeager, CO oxidation on smooth and high area Pt, Pt-Ru and Pt-Sn electrodes, J. Electroanal. Chem., 441 (1998) 77-81.
[49] A.F.B. Barbosa, V. Del Colle, N.A. Galiote, G. Tremiliosi-Filho, Effect of tin deposition over electrogenerated random defects on Pt(111) surfaces onto ethanol electrooxidation: Electrochemical and FTIR studies, J. Electroanal. Chem., 857 (2020) 113734.
[50] M.J.S. Farias, W. Cheuquepán, A.A. Tanaka, J.M. Feliu, Nonuniform synergistic effect of Sn and Ru in site-specific catalytic activity of Pt at bimetallic surfaces toward CO electro-oxidation, ACS Catal., 7 (2017) 3434-3445.